Loss-of-function mutations in IGSF1 cause an X-linked syndrome of central hypothyroidism and testicular enlargement.

ARTICLE *in* NATURE GENETICS · NOVEMBER 2012

Impact Factor: 29.65 · DOI: 10.1038/ng.2453 · Source: PubMed

Loss-of-function mutations in *IGSF1* cause an X-linked syndrome of central hypothyroidism and testicular enlargement

Yu Sun[1,20], Beata Bak[2,20], Nadia Schoenmakers[3,20], A S Paul van Trotsenburg[4,20], Wilma Oostdijk[5], Peter Voshol[3], Emma Cambridge[6], Jacqueline K White[6], Paul le Tissier[7,8], S Neda Mousavy Gharavy[7], Juan P Martinez-Barbera[7], Wilhelmina H Stokvis-Brantsma[5], Thomas Vulsma[4], Marlies J Kempers[4,9], Luca Persani[10,11], Irene Campi[10,12], Marco Bonomi[11], Paolo Beck-Peccoz[10,12], Hongdong Zhu[13], Timothy M E Davis[13], Anita C S Hokken-Koelega[14], Daria Gorbenko Del Blanco[14], Jayanti J Rangasami[15], Claudia A L Ruivenkamp[1], Jeroen F J Laros[1], Marjolein Kriek[1], Sarina G Kant[1], Cathy A J Bosch[1], Nienke R Biermasz[16], Natasha M Appelman-Dijkstra[16], Eleonora P Corssmit[16], Guido C J Hovens[16], Alberto M Pereira[16], Johan T den Dunnen[1,17], Michael G Wade[18], Martijn H Breuning[1], Raoul C Hennekam[4], Krishna Chatterjee[3,21], Mehul T Dattani[19,21], Jan M Wit[5,21] & Daniel J Bernard[2,21]

Congenital central hypothyroidism occurs either in isolation or in conjunction with other pituitary hormone deficits. Using exome and candidate gene sequencing, we identified 8 distinct mutations and 2 deletions in *IGSF1* in males from 11 unrelated families with central hypothyroidism, testicular enlargement and variably low prolactin concentrations. IGSF1 is a membrane glycoprotein that is highly expressed in the anterior pituitary gland, and the identified mutations impair its trafficking to the cell surface in heterologous cells. *Igsf1*-deficient male mice show diminished pituitary and serum thyroid-stimulating hormone (TSH) concentrations, reduced pituitary thyrotropin-releasing hormone (TRH) receptor expression, decreased triiodothyronine concentrations and increased body mass. Collectively, our observations delineate a new X-linked disorder in which loss-of-function mutations in *IGSF1* cause central hypothyroidism, likely secondary to an associated impairment in pituitary TRH signaling.

The index case in family A (A-III.11; **Fig. 1a**) was diagnosed with central hypothyroidism by neonatal screening for congenital hypothyroidism. His cousin (A-III.7), when referred for growth failure at 7.3 years of age, had central hypothyroidism, partial growth hormone (GH) deficiency and low prolactin concentration (**Table 1**). In early adolescence, testicular growth advanced normally in both boys, but testes continued to grow beyond the reference range of testis volume (**Table 1**). In contrast, serum testosterone concentration remained inappropriately low for testicular size until 15.2 and 14.2 years of age, respectively, leading to a late growth spurt and delayed pubic hair development in each. Subsequent testing of the maternal grandfather (A-I.4) showed central hypothyroidism (**Table 1**). X-chromosome exome sequencing in the two cousins (**Supplementary Table 1**) identified a 27-nt deletion, c.2137_2163del (p.Ala713_Lys721del) in *IGSF1* at Xq25 (*IGSF1* reference sequence, NM_001170961.1). The same deletion was present in the grandfather (A-I.4) and another male relative (A-II.4) with the same phenotype (**Fig. 1a** and **Table 1**). Independent whole-exome sequencing

[1]Center for Human and Clinical Genetics, Leiden University Medical Center, Leiden, The Netherlands. [2]Department of Pharmacology and Therapeutics, McGill University, Montréal, Québec, Canada. [3]Institute of Metabolic Science, Metabolic Research Laboratories, Addenbrooke's Hospital, University of Cambridge, Cambridge, UK. [4]Department of Pediatric Endocrinology, Emma Children's Hospital, Academic Medical Center, University of Amsterdam, Amsterdam, The Netherlands. [5]Department of Pediatrics, Leiden University Medical Center, Leiden, The Netherlands. [6]The Sanger Institute Mouse Genetics Project, Wellcome Trust Sanger Institute, Wellcome Trust Genome Campus, Hinxton, Cambridge, UK. [7]Neural Development Unit, University College London (UCL) Institute of Child Health, London, UK. [8]Division of Molecular Neuroendocrinology, National Institute for Medical Research, Mill Hill, London, UK. [9]Department of Human Genetics, Radboud University Nijmegen Medical Center, Nijmegen, The Netherlands. [10]Department of Clinical Sciences & Community Health, Università degli Studi di Milano, Milan, Italy. [11]Division of Endocrine and Metabolic Disorders, Istituto di Ricovero e Cura a Carattere Scientifico (IRCCS), Istituto Auxologico Italiano, Milan, Italy. [12]Endocrine Unit, Fondazione IRCCS Ca'Granda, Milan, Italy. [13]School of Medicine and Pharmacology, Fremantle Hospital Unit, The University of Western Australia, Perth, Western Australia, Australia. [14]Subdivision of Endocrinology, Department of Pediatrics, Erasmus Medical Center–Sophia Children's Hospital, Rotterdam, The Netherlands. [15]Department of Paediatrics, West Middlesex University Hospital, Isleworth, UK. [16]Department of Endocrinology and Metabolic Disorders, Leiden University Medical Center, Leiden, The Netherlands. [17]Leiden Genome Technology Center, Leiden University Medical Center, Leiden, The Netherlands. [18]Hazard Identification Division, Environmental Health Science and Research Bureau, Health Canada, Ottawa, Ontario, Canada. [19]Developmental Endocrinology Research Group, Clinical and Molecular Genetics Unit, UCL Institute of Child Health, London, UK. [20]These authors contributed equally to this work. [21]These authors jointly directed this work. Correspondence should be addressed to J.M.W. (j.m.wit@lumc.nl), D.J.B. (daniel.bernard@mcgill.ca), K.C. (kkc1@medschl.cam.ac.uk) or M.T.D. (m.dattani@ucl.ac.uk).

Received 15 May; accepted 3 October; published online 11 November 2012; doi:10.1038/ng.2453

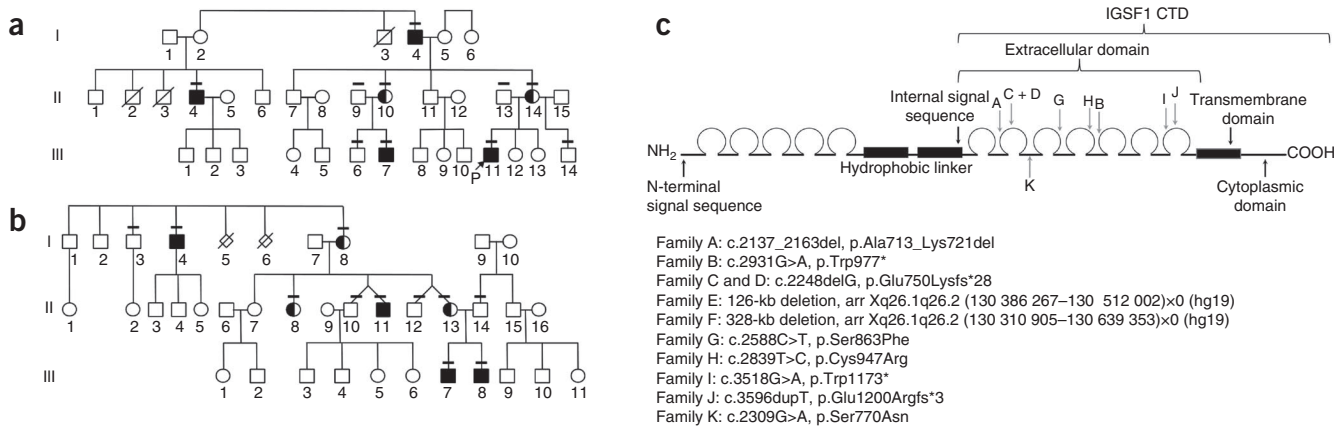

Figure 1 *IGSF1* mutations identified in individuals with central hypothyroidism. (**a**) Pedigree of family A. Small horizontal lines above individuals indicate that the mutation was confirmed. Proband (P) of family A (A-III.11) is indicated by an arrow. (**b**) Pedigree of family B. (**c**) Schematic of the IGSF1 protein domain structure, showing the relative positions of residues affected by the identified mutations (labeled by family). The positions of the deletions in families E and F are not indicated.

of two brothers (B-III.7 and B-III.8) with central hypothyroidism in family B (**Fig. 1b**, **Table 1** and **Supplementary Table 1**) identified a nonsense mutation, c.2931G>A (p.Trp977*), also in *IGSF1* (**Fig. 1c**). B-III.7 and B-III.8 presented in infancy with prolonged neonatal jaundice, but two affected relatives harboring the same mutation were only diagnosed with central hypothyroidism after genetic screening at 65.5 (B-I.4) and 43.3 (B-II.11) years of age (**Fig. 1b**).

We found additional *IGSF1* variants in seven Dutch families (families C–I) and two Italian families (families J and K) characterized by male-specific central hypothyroidism (**Fig. 1c**, **Table 1** and **Supplementary Fig. 1**). Most Dutch and Italian (family J) cases were detected through neonatal screening for congenital hypothyroidism (on the basis of thyroxine (T4) and TSH concentrations). Thyroid function tests at diagnosis are shown in **Supplementary Table 2**. Mean (s.d.)

Table 1 Clinical features of individuals (all males) with *IGSF1* variants

Case	Nucleotide alteration	Amino-acid alteration	Origin	Age at diagnosis of central hypothyroidism	Central hypothyroidism[a]	Prolactin deficiency[b]	Age (years)[c]	Right/left testicular volume (ml) (reference)[d]
A-III.11	c.2137_2163del	p.Ala713_Lys721del	Netherlands	3 weeks	+	–	17.64	21/20 (7.3–16)
A-III.7			Netherlands	7.3 years	+	+	21.36	30/26 (8.5–18.3)
A-II.4			Netherlands	51.5 years	+	–	52.41	32/29 (8.5–18.3)
A-I.4			Netherlands	74.1 years	+	–	67.70	4/large (8.5–18.3)[e]
B-III.7	c.2931G>A	p.Trp977*	UK	4 weeks	+	+	10.52	1.1/1.0 (0.55–1.87)
B-III.8			UK	7 weeks	++	–	7.95	1.8/1.5 (0.45–0.92)
B-II.11			UK	43.3 years	+	+	43.30	68/37 (8.5–18.3)
B-I.4			UK	65.9 years	+	–	66.37	19.6/21.6 (8.5–18.3)
C-III.1	c.2248delG	p.Glu750Lysfs*28	Netherlands	3 weeks	+	+	16.60	18/18 (7.8–16.2)[f]
D-III.3	c.2248delG	p.Glu750Lysfs*28	Netherlands	3 weeks	++	+	10.46	1/1 (0.55–1.87)
D-III.4			Netherlands	1 week	+	+	3.79	0.8/0.8 (0.32–0.70)
D-I.3			Netherlands	61 years	+	–	62.75	21/16 (8.5–18.3)
E-IV.1	126-kb deletion[g]		Netherlands	2 weeks	+	+	20.57	>18/>18 (8.5–18.3)[f]
E-IV.3			Netherlands	2.5 weeks	+	–	22.37	34/25.5 (8.5–18.3)
F-IV.1	328-kb deletion[h]		Netherlands	3 weeks	+	–	12.70	12.2/8.4 (4–13)
F-IV.2			Netherlands	3 weeks	+	+	9.44	1/0.9 (0.5–1.35)
F-II.8			Netherlands	57.5 years	+	+	58.24	44.6/48.2 (8.5–18.3)
G-III.1	c.2588C>T	p.Ser863Phe	Netherlands	5 weeks	+	+	27.52	11.8/38 (8.5–18.3)
G-III.3			Netherlands	2.5 weeks	+	+	23.08	25.5/25.4 (8.5–18.3)
G-I.1			Netherlands	63 years	+	+	87.49	>18/>18 (8.5–18.3)[f]
H-III.2	c.2839T>C	p.Cys947Arg	Netherlands	6.5 years	+	+	18.36	22.7/22.7 (8.5–18.3)
H-III.3			Netherlands	3 weeks	+	+	15.93	21.7/21.7 (6.7–15.3)
I-III.2	c.3518G>A	p.Trp1173*	Netherlands	14.1 years	+	+	16.69	19/17 (8–16.5)
J-III.1	c.3596dupT	p.Glu1200Argfs*3	Italy	3 weeks	+	+	3.26	0.75/0.80 (0.32–0.70)
J-III.2			Italy	2 weeks	+	+	0.16	0.58/0.58 (0.30–0.65)[f]
K-II.3	c.2309G>A	p.Ser770Asn	Italy	10.6 years	+	+	26.54	21.5/21.4 (8.5–18.3)

[a]+, serum FT4 concentration of 50–99% of the lower limit of normal; ++, serum FT4 concentration of <50% of the lower limit of normal. In all cases, serum TSH levels were normal. [b]+, serum prolactin content below the lower limit of normal. [c]Age at sonographic determination of testicular volume. [d]Sonographic testicular volume in comparison to references at the same age[8]. [e]Self-reported unilateral macroorchidism, until the enlarged testis was removed after testicular torsion leading to complete infarction at 74 years. The remaining testis was small and soft, with deficient testosterone secretion. Testosterone treatment was started at 76 years. [f]Estimated on the basis of Prader orchidometer (30 ml by Prader orchidometer = 18.3 ml by ultrasound, 2 ml by Prader orchidometer = 0.58 ml by ultrasound[8]). [g]Arr Xq26.1q26.2 (130386267–130512002)x0 (hg19). [h]Arr Xq26.1q26.2 (130310905–130639353)x0 (hg19).

serum free thyroxine (FT4) concentration was 79% (13%) of the lower limit of the reference range for age and assays. Except for two infants with lower values, all ranged between 67–94% of the reference range. Serum TSH concentrations were within the reference range in all cases (range of 0.8–6.0 mU/l, mean 2.6 mU/l). The FT4/TSH ratio was therefore lower than in controls (3.94 versus 5.73; Mann-Whitney test $P = 0.002$). Mean (s.d.) serum triiodothyronine (T3) concentration in nine 1- to 3-week-old *IGSF1*-deficient infants was 98% (12%) of the lower limit of the reference range for age (range of 83–121%)[1]. In seven older cases, T3 concentration was in the lower half of the reference range. Within families, we observed considerable differences in the extent of hypothyroidism.

In eight infants (2.5–5 weeks old) and eight older subjects (0.4–65.5 years old), standard TRH tests were conducted (**Supplementary Table 2**). In the infants, the peak TSH concentration was 4.5–16.0 mU/l. A similar range was observed in previous reports on congenital central hypothyroidism[2,3], and concentrations are lower than observed in age-matched controls (14–37 mU/l)[3]. At later ages (7.3–63 years), peak TSH concentrations were between 4.3 and 8.5 mU/l, which is in the lower half of the reported reference ranges for males (3.7–12.5 mU/l (ref. 4) or 4.1–13.9 mU/l (ref. 5)). In eight subjects, the increment of serum FT4 (mean (s.d.) = 14.2% (7.9%)) was lower than that reported for controls (mean (s.e.m.) = 23.9% (2.7%)), but the FT3 response to TRH was normal (36.3% versus 41.8% in controls)[6,7] (**Supplementary Table 3**). We could demonstrate central hypothyroidism in 5 of 20 female heterozygous carriers (data not shown).

Serum prolactin concentrations were decreased in 18 of 26 cases (**Table 1**). Cases A-III.7, H-III.3, I-III.2 and K-II.3 showed growth retardation in childhood, associated with biochemical GH insufficiency, and were treated with biosynthetic GH. In young adulthood, GH stimulation tests were normal in the three subjects who had discontinued treatment. Clinical and biochemical details are presented in the **Supplementary Note**. In three cases, magnetic resonance imaging (MRI), performed because of macrocephaly (A-III.11), central hypothyroidism (C-III.1) and GH deficiency (K-II.3), was abnormal, showing a frontoparietal hygroma, hypoplasia of the corpus callosum and small stalk lesion, respectively. In eight other cases, MRIs were normal.

Testicular development showed a characteristic pattern involving normal testicular volume in childhood, increase in testicular volume from approximately 11 years of age onward, while serum testosterone was still low, relatively large testes for serum testosterone (>2 years advance), in adolescence and adult macroorchidism (>30 ml by Prader orchidometer, >18.3 ml by ultrasound)[8] (**Table 1**). No abnormalities were observed in testicular morphology by ultrasound. In 10 out of 11 evaluable cases, testosterone production was delayed, defined as a late increase in serum testosterone concentration (<0.8 nM = <23 ng/dl at 13.0 years)[9] and/or a pubertal growth spurt that was >2 years delayed (compared to Dutch reference data[10]).

The most recent (July 2012) clinical data on height, body mass index (BMI) and pituitary-gonadal hormones for cases are shown in **Table 2**. Mean height was close to the average for population references, but BMI was higher than 25 in 11 out of 13 adults and higher than +2 s.d. score (SDS) in 5 out of 13 children. Plasma testosterone concentration was normal in most cases. A-I.4, who underwent surgery for

Table 2 Clinical and laboratory data

Case	Age (years)	T4 R/	Height SDS[a]	BMI SDS[b]	LH (IU/l)[c]	FSH (IU/l)[c]	LH_{max} to GnRH	FSH_{max} to GnRH	Testosterone (nM)[c]	Inhibin B (ng/l)[d]	AMH (μg/l)[d]
A-III.11	17.64	+	−0.2	2.6	1.0[e]	3.8[e]	13.1[e]	8.3[e]	1.1 (1.0–16.3)[e]	328 (80–300)	16.6 (10–100)
A-III.7	21.36	+	1.0	1.8	3.6	10.6	18.9	18.7	17.6	237	12.4
A-II.4	52.41	–	0.3	2.5	3	17.9	–	–	12.7	199	5.6
A-I.4	86.70	+	0.2	4.3	15[f]	54[f]	–	–	4.8[f]	<10	0.24
B-III.7	10.52	+	1.4	1.9	<1	1.2	–	–	<0.3 (0.2–1.2)	91 (20–300)	97 (30–200)
B-III.8	7.95	+	0.7	2.2	<1	3.1	–	–	<0.3 (0.07–0.31)	111 (20–120)	97 (100–400)
B-II.11	43.29	+	−0.2	3.3	3.7	10.1	29.6	22.6	16.8	279	7.4
B-I.4	66.37	–	−0.6	2.1	2.1	11.0	30.8	36.7	18.7	192	6.2
C-III.1	17.39	+	0.6	2.0	3.2	3.8	–	–	17.2	299 (80–300)	14.0 (10–100)
D-III.3	10.46	+	−0.4	0.8	<1	2.9	1.4	15.4	<0.3 (0.2–1.2)	97 (20–300)	35.4 (30–200)
D-III.4	3.79	+	−0.6	1.1	<1	1.1	–	–	<0.3 (0.07–0.28)	192 (20–100)	207 (100–1,000)
D-I.3	62.75	–	−1.2	7.7	2.5	6.3	22.2	14.1	10.1[7]	152	1.4
E-IV.1	20.57	+	−0.5	1.0	1.3	4.8	–	–	13.4	454	–
E-IV.3	22.37	+	1.0	2.8	4.4	6.0	38.7	13.1	19	317	26.9
F-IV.1	12.70	+	1.1	2.2	<1	2.5	9.4	5.1	4.2 (0.4–9.5)	533 (80–300)	50.2 (10–100)
F-IV.2	9.44	+	1.3	2.9	<1	<1	–	–	1.7 (0.14–0.66)	92 (20–120)	134 (100–400)
F-II.8	58.24	–	1.4	8.6	3.5	8.6	21	15.3	5.1[g]	141	5.2
G-III.1	27.52	+	−0.5	3.5	3.8	3.9	25	7.8	24	249	4.5
G-III.3	23.08	+	0.6	1.5	3.2	6.9	31.8	17.2	24	249	5.9
G-I.1	87.49	+	−1.9	2.5	–	–	–	–	–	–	–
H-III.2	20.52	+	−2.5	2.6	2.7	4.6	–	–	11.8	338	7.2
H-III.3	18.09	+	−0.7	1.7	6.5	10.7	–	–	16.9	265	6.4
I-III.2	16.69	+	−0.6	2.0	<1	3.9	14.3	9.8	9.5 (1.7–27.8)	257 (80–300)	3.3 (10–100)
J-III.1	3.26	+	0.1	1.0	–	–	–	–	–	–	–
J-III.2	0.16	+	0.5	1.4	–	–	–	–	–	–	–
K-II.3	26.54	+	0.1	1.1	1.6	3.4	36.5	10.7	11.5	284	10.8

T4 R/, L-thyroxine treatment; IU, International Units.
[a]Height is expressed as s.d. score (SDS) for national reference data for The Netherlands[23], UK[24] and Italy[25]. The mean (s.d.) height is 0.0 (1.0) SDS. [b]BMI is expressed as SDS for Dutch references obtained in 1980 (ref. 26). Median BMI = 2.1 SDS. [c]Reference ranges for males of >17 years: testosterone of 11–35 nM, LH < 0.1–15 IU/l and FSH < 0.1–10 IU/l. Reference ranges for testosterone in boys (10th to 90th percentile) according to von Schnakerburg *et al.*[27]. [d]Reference range for males of >18 years: inhibin B of 150–400 ng/l and AMH of 5–30 μg/l. Reference ranges for younger age groups are indicated. [e]GnRH test and testosterone performed at 15.19 years, before start of testosterone substitution therapy. [f]LH, FSH and testosterone concentrations before the start of testosterone substitution therapy (at 76 years). [g]Because of low plasma SHBG concentration, free androgen index (FA = (100 × testosterone)/SHBG) was high in D-I.3 (67 years, age reference 18–54 years) and normal in F-II.8 (46 years, age reference 30–53 years).

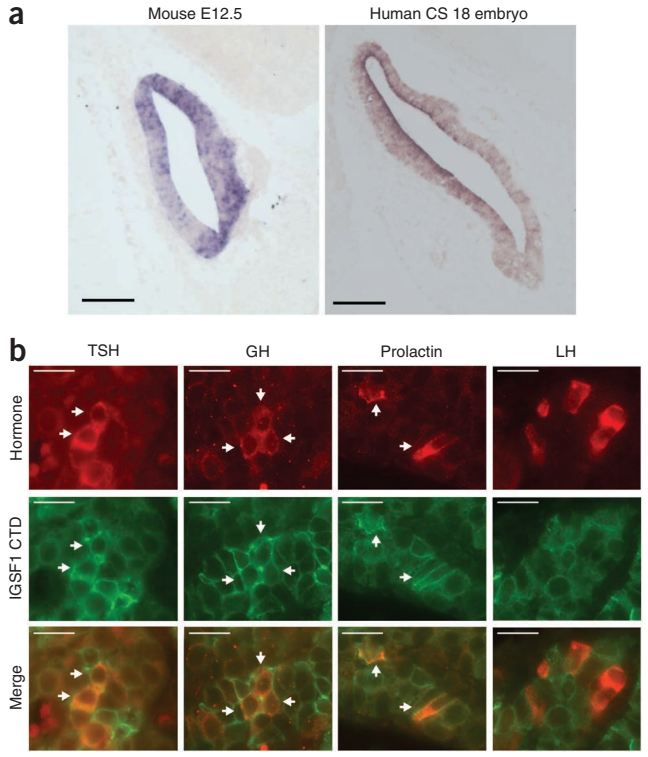

Figure 2 IGSF1 is expressed in anterior pituitary gland. (**a**) Expression of *Igsf1* mRNA in mouse embryonic day (E) 12.5 embryo and *IGSF1* mRNA in human embryo Carnegie stage 18 Rathke's pouch progenitors as detected by *in situ* hybridization. Scale bars, 10 µm. (**b**) Immunofluorescence using antibodies against the IGSF1 CTD and the indicated anterior pituitary hormones (TSH, thyrotropes; GH, somatotropes; prolactin, lactotropes; LH, gonadotropes) was performed in wild-type E18.5 mouse pituitary. Arrows indicate colocalization of IGSF1 CTD and hormone signal. Scale bars, 10 µm.

testicular torsion and in whom the remaining testis was atrophic, had low testosterone concentration and elevated gonadotropins before the start of testosterone substitution, and, currently, at the age of 86.7 years, his inhibin B and anti-Müllerian hormone (AMH) concentrations are very low. The two subjects with severe obesity (D-I.3 and F-II.8) had low plasma testosterone concentrations, but, because of low plasma sex hormone–binding globulin (SHBG) concentration, the free androgen index was normal. Plasma luteinizing hormone (LH), follicle stimulating hormone (FSH), inhibin B and AMH concentrations were within reference ranges in the majority of cases, but plasma FSH concentration was always higher than LH concentration and was above the reference range in six cases. The response to gonadotropin-releasing hormone (GnRH) (100 µg administered intravenously) was higher for LH than for FSH concentration in all except two subjects. Inhibin B concentration tended to be high (elevated in four subjects), and AMH concentration was relatively low (decreased in five subjects) relative to the reference range. Serum high-density lipoprotein (HDL) and low-density lipoprotein (LDL) cholesterol, triglyceride, glucose, insulin and C-peptide concentrations did not indicate the presence of a metabolic syndrome (data not shown).

The identified *IGSF1* mutations are summarized in **Figure 1c**. Families C and D harbored the same single-nucleotide deletion (c.2248delG (p.Glu750Lysfs*28)). In families E and F, we observed submicroscopic gene deletions of different sizes that affected *IGSF1* and no other annotated gene. Affected members of families G–I and K had missense or nonsense mutations, and there was a single-nucleotide duplication (c.3596dupT (p.Glu1200Argfs*3)) in family J. All variants were confirmed by Sanger sequencing (**Supplementary Table 4**), map to conserved regions of the gene, are not present in available databases (dbSNP, 1000 Genomes Project, the Leiden Open Variance Database (LOVD), the Human Gene Mutation Database (HGMD) and Genome of the Netherlands (GoNL, pilot data of 500 unrelated individuals)) and were not previously reported.

IGSF1 encodes a plasma membrane immunoglobulin superfamily glycoprotein[11,12]. The canonical IGSF1 protein has 12 C2-type immunoglobulin loops, a transmembrane domain and a short intracellular C tail (**Fig. 1c**). A hydrophobic linker separating immunoglobulin loops 5 and 6 targets the protein for obligate cotranslational proteolysis, such that only the C-terminal domain (CTD) traffics to the plasma membrane[13]. Human *IGSF1* and mouse *Igsf1* mRNAs are abundantly expressed in Rathke's pouch (the developing pituitary primordium; **Fig. 2a**) and in adult pituitary gland and testis[13–17] (**Supplementary Fig. 2).** IGSF1 protein is detected in mouse thyrotropes, somatotropes and lactotropes but not in gonadotropes (**Fig. 2b**) or in testis (data not shown).

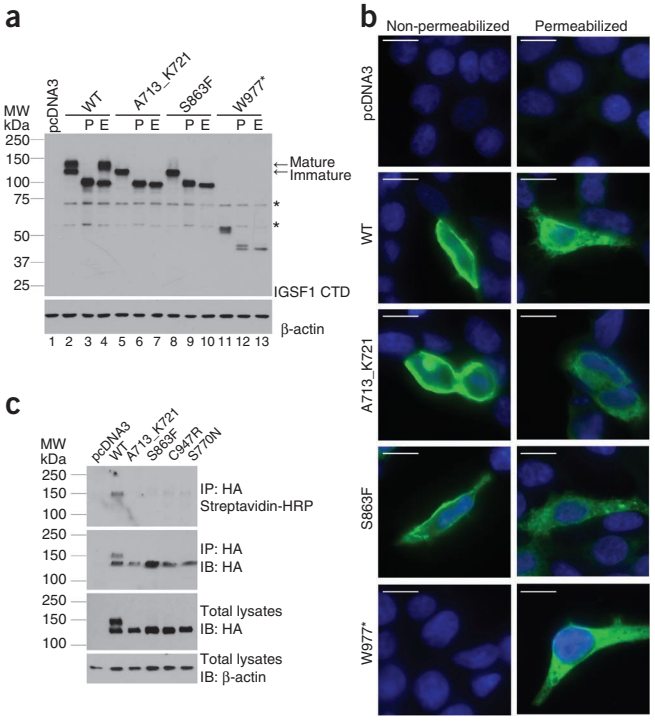

Figure 3 Alterations in IGSF1 impair its plasma membrane trafficking. (**a**) HEK293 cells were transfected with pcDNA3 (empty vector) or with vectors expressing the indicated wild-type (WT) and mutant IGSF1 proteins. Protein lysates were deglycosylated with either PNGaseF (P) or EndoH (E), resolved by SDS-PAGE and immunoblotted using an antibody specific to the IGSF1 CTD. Non-specific bands are indicated with an asterisk. MW, molecular weight. (**b**) HEK293 cells were transfected with the same constructs as in **a**. Expression of the IGSF1 CTD was analyzed by immunofluorescence using the antibody against IGSF1 CTD under non-permeabilizing and permeabilizing conditions. Nuclei were stained with DAPI (blue). Scale bars, 10 µm. (**c**) HEK293 cells were transfected with pcDNA3 or with vectors expressing the indicated wild-type and mutant IGSF1 proteins. Membrane expression of IGSF1 CTD was analyzed by cell surface biotinylation. IB, immunoblot; IP, immunoprecipitation; HRP, horseradish peroxidase.

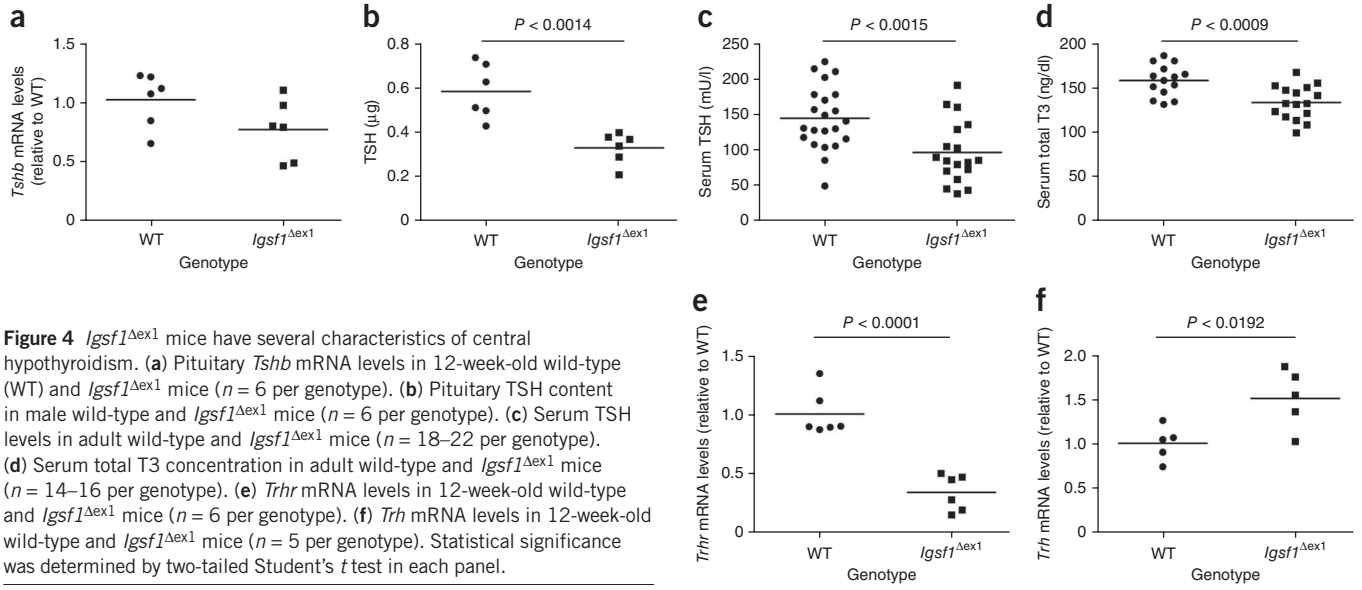

Figure 4 *Igsf1*$^{\Delta ex1}$ mice have several characteristics of central hypothyroidism. (**a**) Pituitary *Tshb* mRNA levels in 12-week-old wild-type (WT) and *Igsf1*$^{\Delta ex1}$ mice ($n = 6$ per genotype). (**b**) Pituitary TSH content in male wild-type and *Igsf1*$^{\Delta ex1}$ mice ($n = 6$ per genotype). (**c**) Serum TSH levels in adult wild-type and *Igsf1*$^{\Delta ex1}$ mice ($n = 18–22$ per genotype). (**d**) Serum total T3 concentration in adult wild-type and *Igsf1*$^{\Delta ex1}$ mice ($n = 14–16$ per genotype). (**e**) *Trhr* mRNA levels in 12-week-old wild-type and *Igsf1*$^{\Delta ex1}$ mice ($n = 6$ per genotype). (**f**) *Trh* mRNA levels in 12-week-old wild-type and *Igsf1*$^{\Delta ex1}$ mice ($n = 5$ per genotype). Statistical significance was determined by two-tailed Student's *t* test in each panel.

The phenotypes of cases with intragenic mutations are highly similar to those of individuals with complete *IGSF1* deletion (families E and F) (**Table 1**), suggesting loss of IGSF1 function in all cases. The identified mutations in families A–D and G–K map to the IGSF1 CTD coding region (**Fig. 1c**). We therefore examined expression and post-translational regulation of IGSF1 mutants in heterologous HEK293 cells. Wild-type IGSF1 migrated as a doublet of 140–150 kDa in protein blot analysis (**Fig. 3a**, lane 2), reflecting the mature N-glycosylated and immature endoplasmic reticulum (ER)-resident forms of the CTD (**Fig. 3a**, lanes 3 and 4)[13]. In contrast, IGSF1 Ala713_Lys721del (family A; primer sequences are given in **Supplementary Table 5**) migrated predominantly as an immature form (**Fig. 3a**, lanes 5–7). Similar migratory patterns were observed for IGSF1 Ser863Phe (family G; **Fig. 3a**; lanes 8–10) and the other two missense mutants (Cys947Arg (family H) and Ser770Asn (family K); **Supplementary Fig. 3a**, lanes 6–11). The nonsense mutants in families B and I (p.Trp977*; **Fig. 3a**, lanes 11–13; p.Trp1173*, **Supplementary Fig. 3a**, lanes 17–19) and frameshift mutants in families C and D (p.Glu750Lysfs*28) and J (p.Glu1200Argfs*3) (**Supplementary Fig. 3a**, lanes 3–5 and 12–14) possessed immature sugars and were truncated relative to wild-type IGSF1. On the basis of their patterns of glycosylation, the identified IGSF1 mutants appeared to be retained in the ER.

To assess plasma membrane trafficking, we transfected HEK293 cells with constructs encoding wild-type and mutant IGSF1 and detected the expressed proteins by immunofluorescence with an antibody directed against the N terminus of the IGSF1 CTD. Membrane staining was observed in non-permeabilized cells transfected with the construct for wild-type IGSF1 (**Fig. 3b**). A similar pattern was observed with IGSF1 Ala713_Lys721del and the three missense mutants (**Fig. 3b** and **Supplementary Fig. 3b**); however, cell surface biotinylation showed that mutant proteins reached the plasma membrane with poor efficiency and with distinct glycosylation patterns compared to wild-type protein (**Fig. 3c**). Membrane signals were never detected in non-permeabilized cells transfected with vectors expressing IGSF1 p.Trp977* (**Fig. 3b**) or the other truncated forms of the protein (**Supplementary Fig. 3b**). We did not detect secreted proteins in the culture medium (data not shown). In contrast, we observed a strong intracellular staining pattern in permeabilized cells with all constructs (**Fig. 3b** and **Supplementary Fig. 3b**), confirming expression of the mutant proteins. Thus, the identified mutations block or substantially impair IGSF1 CTD plasma membrane trafficking.

To establish a causal link between loss of IGSF1 function and central hypothyroidism, we examined pituitary and thyroid function in *Igsf1*-deficient mice[17] (**Supplementary Fig. 4**). mRNA levels for various pituitary hormone-encoding genes, including *Tshb*, did not differ between control and *Igsf1*-deficient mice (**Fig. 4a** and **Supplementary Fig. 5a**). In contrast, both pituitary and serum TSH content was significantly reduced in adult *Igsf1*-deficient males (**Fig. 4b**,**c**). Pituitary prolactin content was unaffected (**Supplementary Fig. 5b**). Whereas circulating T3 concentrations were decreased in *Igsf1*-deficient males (**Fig. 4d**), T4/FT4 concentrations were similar to those of controls in the majority of cases, and thyroid histology appeared normal (**Supplementary Fig. 5c**,**d** and data not shown). Reduced TSH synthesis and secretion (**Fig. 4b**,**c**) in spite of normal *Tshb* mRNA expression (**Fig. 4a**) in *Igsf1*-deficient mouse pituitaries suggested impaired TRH signaling. Consistent with this idea, pituitary *Trhr* mRNA levels were reduced, and hypothalamic *Trh* mRNA levels were increased, in *Igsf1*-deficient mice relative to controls (**Fig. 4e**,**f**). Pituitary *Gnrhr* mRNA expression was not altered (data not shown). Finally, *Igsf1*-deficient males were heavier than their control littermates (29.9 ± 0.4 versus 28.2 ± 0.3 g at 12 weeks; $P = 0.004$). Thus, adult male *Igsf1*-deficient mice display several characteristics of central hypothyroidism.

IGSF1 was initially hypothesized to function as a pituitary inhibin coreceptor[15,18,19], raising the possibility that macroorchidism in our cases might be linked to loss of inhibin activity and, therefore, enhanced FSH secretion. However, the putative role of IGSF1 as an inhibin coreceptor has been challenged by more recent binding and *in vivo* data[17,19]. In our cases, serum FSH concentration was higher than that of LH but exceeded the reference range in only six cases (**Table 2**). Moreover, male *Igsf1*-deficient mice are fertile and have normal testicular size and FSH concentration (ref. 17 and **Supplementary Fig. 5a**,**e**). Therefore, at present, the mechanisms of testicular enlargement in our cases are unresolved.

In summary, our data delineate a new X-linked disorder in which loss-of-function mutations in *IGSF1* cause central hypothyroidism, testicular enlargement and variable prolactin and GH deficiency. The identified human *IGSF1* defects impair either expression or membrane trafficking of the IGSF1 CTD, consistent with a loss of protein function.

Igsf1 deletion decreases pituitary and circulating TSH content in mice, perhaps secondary to impaired TRH receptor signaling. Loss of IGSF1 function was associated with profound hypothyroxinemia in some cases, with the attendant risk of neurodevelopmental delay, if untreated. In other cases, hypothyroxinemia was less severe, but untreated subclinical hypothyroidism is associated with adverse cardiometabolic risk, which can be reversed by thyroxine treatment[20–22]. Thus, following genetic ascertainment of future cases, biochemical screening and thyroxine treatment of affected family members will be of substantial clinical benefit. Collectively, our observations uncover a completely unexpected and clinically relevant role for IGSF1 in pituitary and testicular function.

URLs. RefSeq, http://www.ncbi.nlm.nih.gov/RefSeq/; dbSNP, http://www.ncbi.nlm.nih.gov/projects/SNP/; 1000 Genomes Project, http://www.1000genomes.org/; HapMap Project, http://hapmap.ncbi.nlm.nih.gov/; UniProt, http://www.uniprot.org/; Human Splicing Finder, http://www.umd.be/HSF/; BWA, http://bio-bwa.sourceforge.net/; SAMtools, http://samtools.sourceforge.net/; GMAP, http://research-pub.gene.com/gmap/; SeattleSeq Annotation, http://snp.gs.washington.edu/SeattleSeqAnnotation131/; SIFT, http://sift.jcvi.org/; PolyPhen-2, http://genetics.bwh.harvard.edu/pph2/; LOVD IGSF1 database, http://www.lovd.nl/igsf1.

METHODS

Methods and any associated references are available in the online version of the paper.

Accession codes. X-chromosome sequencing data were deposited at the LOVD3 database: http://databases.lovd.nl/shared/individuals/00000208 and http://databases.lovd.nl/shared/individuals/00000209.

Note: Supplementary information is available in the online version of the paper.

ACKNOWLEDGMENTS

The authors thank X.-H. Liao from the Refetoff laboratory (The University of Chicago, supported by US National Institutes of Health (NIH) grant DK15700) for measuring T4, T3, FT4I and TSH in mice, P. Scheiffele for the antibody to IGSF1 CTD and S. Kimmins (McGill University) and P. Bisschop (Academic Medical Center, University of Amsterdam) for human testis and pituitary RNA, respectively. We also thank H. Bikker, J.C. Moreno, A. Escudero, E. Aten, M. Losekoot, E. Endert, J.W.A. Smit, R.van Rijn and E.L. van Persijn-van Meerten for technical support and advice. We thank F.J. de Jong and Y. de Rijke for measuring serum inhibin B and AMH and for providing age references. We thank S. Tran and X. Zhou for assistance with collection of mouse serum samples. We acknowledge the help of N. Zwaveling, J. Gosen, E.J. Schroor, L.C.G. de Graaff and G. Radetti in providing clinical data. We acknowledge The Eastern Region Sequencing and Informatics Hub (see URLs), who undertook sequencing and preliminary bioinformatics analyses of data from the UK families. We thank the subjects and their families for participating. Our work was supported in part by a grant from the China Scholarship Council (to Y.S.); a National Sciences and Engineering Research Council (NSERC) Doctoral Research Award (to B.B.), NSERC Discovery Grant 341801-07 and a Fonds de la Recherche en Santé du Québec (FRSQ) Chercheur Boursier Senior Award (to D.J.B.); grants from the Wellcome Trust (095564 to N.S. and K.C.; WT077157/Z/05/Z to E.C. and J.K.W.; 084361, 078432 and 086545 to J.P.M.-B.), the National Institutes of Health Research Cambridge Biomedical Research Centre (to N.S. and K.C.) and the UK Medical Research Council (MRC; U117570590 to P.l.T.); a National Health and Medical Research Council of Australia Practitioner Fellowship (to T.M.E.D.); the Dutch Growth Research Foundation (D.G.D.B.); the Young Investigator grant of the Italian Ministry of Health and Istituto Auxologico Italiano IRCCS (GR-2008-1137632 to M.B.); and the Great Ormond Street Children's Hospital Charity (to M.T.D.).

AUTHOR CONTRIBUTIONS

Y.S., J.T.d.D., M.K., N.S. and K.C. developed the exome sequencing protocol. A.S.P.v.T., W.O., S.G.K., N.R.B., N.M.A.-D., A.M.P., M.H.B., R.C.H., M.T.D., N.S., L.P., I.C., M.B., P.B.-P., H.Z., T.M.E.D., K.C., A.C.S.H.-K., D.G.D.B. and J.M.W. designed the clinical research studies. Y.S., J.F.J.L. and N.S. performed bioinformatics analyses, mutational analysis and genotyping. B.B. generated the vectors expressing mutant IGSF1 and performed all associated biochemical analyses; maintained the mouse colony, collected all mouse tissues and plasma, and analyzed pituitary gene expression; and prepared figures. D.J.B. generated the mouse model, supervised all *in vitro* and mouse work and participated in data collection and construction of the figures. P.V. and M.G.W. contributed to mouse phenotyping. E.C., J.K.W. and M.G.W. performed mouse T4 measurements. P.l.T. performed measurements of pituitary TSH and prolactin content. S.N.M.G. and J.P.M.-B. carried out the IGSF1 expression studies in mouse and human embryos. C.A.L.R. and C.A.J.B. performed and analyzed the microarray and hybridization experiments. A.S.P.v.T., W.O., W.H.S.-B., T.V., M.J.K., L.P., I.C., M.B., P.B.-P., H.Z., T.M.E.D., A.C.S.H.-K., D.G.D.B., J.J.R., S.G.K., N.R.B., N.M.A.-D., A.M.P., G.C.J.H., E.P.C., M.H.B., R.C.H., A.C.S.H.-K. and M.T.D. contributed to clinical evaluations and the delineation of the subject phenotypes. Y.S., B.B., N.S., A.S.P.v.T., K.C., M.T.D., R.C.H., D.J.B. and J.M.W. prepared the manuscript. D.J.B., J.M.W., K.C. and M.T.D. conceived and supervised the study.

COMPETING FINANCIAL INTERESTS

The authors declare no competing financial interests.

Published online at http://www.nature.com/doifinder/10.1038/ng.2453.
Reprints and permissions information is available online at http://www.nature.com/reprints/index.html.

1. Elmlinger, M.W., Kuhnel, W., Lambrecht, H.G. & Ranke, M.B. Reference intervals from birth to adulthood for serum thyroxine (T4), triiodothyronine (T3), free T3, free T4, thyroxine binding globulin (TBG) and thyrotropin (TSH). *Clin. Chem. Lab. Med.* **39**, 973–979 (2001).
2. Mehta, A. *et al.* Is the thyrotropin-releasing hormone test necessary in the diagnosis of central hypothyroidism in children. *J. Clin. Endocrinol. Metab.* **88**, 5696–5703 (2003).
3. van Tijn, D.A., de Vijlder, J.J. & Vulsma, T. Role of the thyrotropin-releasing hormone stimulation test in diagnosis of congenital central hypothyroidism in infants. *J. Clin. Endocrinol. Metab.* **93**, 410–419 (2008).
4. Faglia, G. *et al.* Plasma thyrotropin response to thyrotropin-releasing hormone in patients with pituitary and hypothalamic disorders. *J. Clin. Endocrinol. Metab.* **37**, 595–601 (1973).
5. Crofton, P.M., Tepper, L.A. & Kelnar, C.J. An evaluation of the thyrotrophin-releasing hormone stimulation test in paediatric clinical practice. *Horm. Res.* **69**, 53–59 (2008).
6. Persani, L. *et al.* Evidence for the secretion of thyrotropin with enhanced bioactivity in syndromes of thyroid hormone resistance. *J. Clin. Endocrinol. Metab.* **78**, 1034–1039 (1994).
7. Persani, L., Ferretti, E., Borgato, S., Faglia, G. & Beck-Peccoz, P. Circulating thyrotropin bioactivity in sporadic central hypothyroidism. *J. Clin. Endocrinol. Metab.* **85**, 3631–3635 (2000).
8. Goede, J. *et al.* Normative values for testicular volume measured by ultrasonography in a normal population from infancy to adolescence. *Horm. Res. Paediatr.* **76**, 56–64 (2011).
9. Dattani, M.T., Tziaferi, V. & Hindmarsh, P.C. Evaluation of disordered puberty. in *Brook's Clinical Pediatric Endocrinology* (eds. Brook, C.G.D., Clayton, P.E. & Brown, R.S.), 213–238 (Wiley-Blackwell, Oxford, 2009).
10. Mul, D. *et al.* Pubertal development in The Netherlands 1965–1997. *Pediatr. Res.* **50**, 479–486 (2001).
11. Mazzarella, R., Pengue, G., Jones, J., Jones, C. & Schlessinger, D. Cloning and expression of an immunoglobulin superfamily gene (*IGSF1*) in Xq25. *Genomics* **48**, 157–162 (1998).
12. Frattini, A., Faranda, S., Redolfi, E., Allavena, P. & Vezzoni, P. Identification and genomic organization of a gene coding for a new member of the cell adhesion molecule family mapping to Xq25. *Gene* **214**, 1–6 (1998).
13. Robakis, T., Bak, B., Lin, S.H., Bernard, D.J. & Scheiffele, P. An internal signal sequence directs intramembrane proteolysis of a cellular immunoglobulin domain protein. *J. Biol. Chem.* **283**, 36369–36376 (2008).
14. Su, A.I. *et al.* A gene atlas of the mouse and human protein-encoding transcriptomes. *Proc. Natl. Acad. Sci. USA* **101**, 6062–6067 (2004).
15. Chong, H. *et al.* Structure and expression of a membrane component of the inhibin receptor system. *Endocrinology* **141**, 2600–2607 (2000).
16. Bernard, D.J. & Woodruff, T.K. Inhibin binding protein in rats: alternative transcripts and regulation in the pituitary across the estrous cycle. *Mol. Endocrinol.* **15**, 654–667 (2001).
17. Bernard, D.J., Burns, K.H., Haupt, B., Matzuk, M.M. & Woodruff, T.K. Normal reproductive function in InhBP/p120-deficient mice. *Mol. Cell. Biol.* **23**, 4882–4891 (2003).
18. Chapman, S.C. & Woodruff, T.K. Modulation of activin signal transduction by inhibin B and inhibin-binding protein (INhBP). *Mol. Endocrinol.* **15**, 668–679 (2001).

19. Chapman, S.C., Bernard, D.J., Jelen, J. & Woodruff, T.K. Properties of inhibin binding to betaglycan, InhBP/p120 and the activin type II receptors. *Mol. Cell. Endocrinol.* **196**, 79–93 (2002).
20. Razvi, S. *et al.* The beneficial effect of L-thyroxine on cardiovascular risk factors, endothelial function, and quality of life in subclinical hypothyroidism: randomized, crossover trial. *J. Clin. Endocrinol. Metab.* **92**, 1715–1723 (2007).
21. Singh, S. *et al.* Impact of subclinical thyroid disorders on coronary heart disease, cardiovascular and all-cause mortality: a meta-analysis. *Int. J. Cardiol.* **125**, 41–48 (2008).
22. Doin, F.C., Rosa-Borges, M., Martins, M.R., Moises, V.A. & Abucham, J. Diagnosis of subclinical central hypothyroidism in patients with hypothalamic-pituitary disease by Doppler echocardiography. *Eur. J. Endocrinol.* **166**, 631–640 (2012).
23. Fredriks, A.M. *et al.* Continuing positive secular growth change in The Netherlands 1955–1997. *Pediatr. Res.* **47**, 316–323 (2000).
24. Freeman, J.V. *et al.* Cross sectional stature and weight reference curves for the UK, 1990. *Arch. Dis. Child.* **73**, 17–24 (1995).
25. Cacciari, E. *et al.* Italian cross-sectional growth charts for height, weight and BMI (2 to 20 yr). *J. Endocrinol. Invest.* **29**, 581–593 (2006).
26. Cole, T.J. & Roede, M.J. Centiles of body mass index for Dutch children aged 0–20 years in 1980—a baseline to assess recent trends in obesity. *Ann. Hum. Biol.* **26**, 303–308 (1999).
27. von Schnakenburg, K., Bidlingmaier, F. & Knorr, D. 17-hydroxyprogesterone, androstenedione, and testosterone in normal children and in prepubertal patients with congenital adrenal hyperplasia. *Eur. J. Pediatr.* **133**, 259–267 (1980).

ONLINE METHODS

DNA isolation. DNA was isolated from human whole blood using the Autopure LS system (Qiagen) and associated reagents, following the manufacturer's protocol. All participants provided written informed consent. The study was approved by the ethics committees of Leiden University Medical Center (Leiden, The Netherlands), Academic Medical Center (Amsterdam, The Netherlands), Anglia and Oxford MREC (Cambridge, UK), Great Ormond Street Hospital (London, UK), Erasmus University Medical Center (Rotterdam, The Netherlands) and the IRCCS Istituto Auxologico Italiano (Milan, Italy).

Exome enrichment and next-generation sequencing. X-chromosome exome enrichment was carried out using Agilent's SureSelect X chromosome oligonucleotide capture library according to the manufacturer's protocol, except that DNA was hybridized with half of the amount of suggested probe. Illumina Genome Analyzer IIx sequencing generated 51-bp paired-end reads. An overview of reads is shown in **Supplementary Table 1**. Whole-exome sequencing was undertaken using the SureSelect Human All Exon 50Mb kit (Agilent Technologies). Sequencing was performed with the SOLiD 4 system (Applied Biosystems).

Read mapping, variant calling and annotation. For the X-chromosome exome data, reads were aligned to reference genome hg19 by Burrows-Wheeler Aligner (BWA) 0.5.8 (ref. 28). BAM file manipulation and variant (single-nucleotide variant (SNV) and insertion and/or deletion (indel)) calling was performed with SAMtools 0.1.9 (ref. 29). The deletion in family A was detected by GMAP v3. 2011-03-28 (alignment)[30] and SAMtools 0.1.9 (variant calling). SeattleSeq Annotation 131 was applied to annotate all variants. Variants in dbSNP131 and the 1000 Genomes Project were filtered out for mutation screening. Whole-exome experiments, sequencing and preliminary analyses were undertaken at the Eastern Region Sequencing and Informatics Hub using the Genome Analysis Toolkit[31].

Filtering strategy. In family A, variants shared by both boys were classified on the basis of their function; only exonic and splice-site variants were taken forward. We then filtered out all variants present in the local, in-house exome sequencing database, dbSNP, 1000 Genomes Project, LOVD and HapMap Project with an allele frequency of >1% in populations of European ancestry, which yielded no promising results. We therefore examined the variant list generated by GMAP and SAMtools, as GMAP allows gap alignment and enables identification of larger insertions and deletions. The same filtering procedure was applied on these variants. For family B, we compared variants from the two brothers; only shared exonic and splice-site variants were taken forward to the filtering step. We filtered out all variants present in databases and the UK 10K genomes project and focused on previously unknown, shared homozygous or X-linked hemizygous variants, using public databases to identify plausible candidates.

Sanger sequence analysis. PCR was performed using Phire Hot Start II DNA polymerase (Finnzyme) following the manufacturer's protocol (primer sequences are listed in **Supplementary Table 4**). Products were purified with the QIAquick PCR purification kit (Qiagen) and mixed with 10 pmol of forward or reverse primer and sequenced with the Applied Biosystems 96-capillary 3730xl system.

Microarrays. We performed analysis on the cytogenetic whole-genome 2.7M array (Affymetrix) according to the manufacturer's protocol. In families C and D, this analysis identified the same haploblock of 23 Mb around the deletion (rs929590 to rs16979902), suggesting a common ancestral origin for these families, although no familial relationship is known for at least four generations.

Expression constructs. The epitope for the antibody to IGSF1 CTD encoded by the human Myc-IGSF1-HA construct (from P. Scheiffele) was modified (QuikChange, Stratagene) to match the mouse protein to facilitate detection with polyclonal antibody against IGSF1 CTD (P. Scheiffele). Mutations were introduced into the construct using QuikChange or Phusion (Thermo; to create the p.Ala713_Lys721del alteration) site-directed mutagenesis (primer sequences are listed in **Supplementary Table 5**). Constructs were verified by sequencing (McGill University and Genome Québec Innovation Centre).

Cell culture. For protein blotting and cell surface biotinylation, HEK293 cells were plated in 6-well plates and transfected with 200 ng of expression vector using Lipofectamine 2000 (Invitrogen) following the manufacturer's instructions. For immunofluorescence, HEK293 cells were plated in 24-well plates on glass coverslips with 50,000 cells per well and transfected with 100 ng of expression vector.

Protein blotting. Whole-cell extracts were prepared from transfected cells 24 h after transfection using RIPA buffer (150 mM NaCl, 50 mM sodium fluoride, 10 mM $NaPO_4$, 2 mM EDTA, 1% NP-40, 1% sodium deoxycholate, 0.1% SDS). Protein lysates were deglycosylated with PNGaseF and EndoH (New England Biolabs), according to the manufacturer's instructions. Protein blots were performed as previously described[32].

Cell immunofluorescence. Under non-permeabilizing conditions, antiserum to IGSF1 CTD (1:500 dilution in serum-free DMEM) was applied to cells for 2 h at 37 °C in 5% CO_2. Cells were transferred to room temperature, washed three times with serum-free DMEM and fixed with 4% paraformaldehyde (PFA). Cells were then washed three times with PBS and incubated in 5% BSA in PBS for 1 h. Secondary antibody (1:600 dilution in 5% BSA in PBS) was applied to cells for 1 h, and cells were washed three times with PBS and mounted using aqueous medium with DAPI. Under permeabilizing conditions, cells were fixed using 4% PFA, washed three times in PBS, incubated in 0.3% Triton X-100 in PBS (PBSX) and incubated in 5% BSA in PBSX for 1 h. Antiserum to IGSF1 CTD (1:500 dilution in 5% BSA in PBSX) was applied to cells for 2 h. Cells were washed three times with PBS. Secondary antibody (1:600 dilution in 5% BSA in PBSX) was applied for 1 h, and cells were washed three times with PBS and mounted under non-permeabilizing conditions.

Pituitary immunofluorescence. The morning when a vaginal plug was detected was considered E0.5. Pregnant mice at E18.5 were sacrificed, and embryo heads were fixed overnight in 4% PFA at 4 °C and embedded in paraffin, with sections sliced with 5 µm thickness. Sections were treated as previously described[33]. Nonspecific binding was blocked using 5% BSA in PBS with 0.2% Tween-20 (PBST). Sections were incubated with primary antibodies (IGSF1 CTD, 1:500 dilution, and (from Santa Cruz Biotechnology) TSH (sc7815) and LH (sc7824), 1:400 dilution, and GH (sc10365) and prolactin (sc7805) 1:200 dilution, in blocking buffer) overnight at 4 °C. Sections were washed three times with PBST, incubated in biotin-conjugated horse secondary antibody to goat (1:150 dilution in blocking buffer) for 1 h, washed three times with PBST, incubated in Streptavidin–Texas Red (1:400 dilution in blocking buffer) and Alexa 488–conjugated goat secondary antibody to rabbit (1:600 dilution) for 1 h, washed three times with PBST and mounted.

Cell surface biotinylation. Transfected cells were washed three times with PBS and incubated in 1 ml of 0.5 mg/ml EZ-link-sulfo-NHS-LC-biotin (Thermo) for 30 min at 4 °C, washed three times with 100 mM glycine in PBS, harvested in lysis buffer (50 mM Tris, pH 7.5, 150 mM NaCl, 1 mM EDTA, 1% Triton X-100) and lysed by sonication (9 W for 10 s). Lysates were centrifuged, supernatant was collected and immunoprecipitation was carried out using EZview anti-HA affinity gel (E6779, Sigma) according to the manufacturer's instructions. Lysates were then processed for protein blotting. After blocking, membrane was incubated in 2.5% milk in TBST with two drops each of A and B reagents from the Vectastain kit (Vector) for 30 min. Membrane was washed three times with 10-min washes in TBST, and signal was visualized using the Western Lightning Plus-ECL kit (PerkinElmer).

Animals. *Igsf1*-deficient mice have been described previously[17]. Tissue and blood collection was performed in accordance with institutional (McGill University) and federal guidelines.

***In situ* hybridization.** *In situ* hybridization was performed as previously described[34] using riboprobes from human *IGSF1* cDNA clone 30387876 (IMAGE). Human embryonic material was provided by the Human Developmental Biology Resource, supported by Medical Research Council Grant G0700089 and Wellcome Trust Grant 082557.

doi:10.1038/ng.2453

RNA blotting. Human pituitary RNA was from the Netherlands Brain Bank (NBB; 02-055) and was obtained in accordance with formal permission for a brain autopsy and use of human brain material and clinical information for research purposes. Human testicular RNA was obtained from S. Kimmins. Each RNA (13 μg) was blotted as previously described[17], using a probe spanning exons 18–20 of mouse *Igsf1*.

Hormone concentration measurements. At diagnosis, serum FT4, TSH, T3 and prolactin concentrations were determined in the laboratories of the participating departments. At follow-up, samples were investigated in the Endocrine Laboratory at Erasmus Medical Center (inhibin B and AMH) and the Laboratory of Endocrinology and Radiochemistry at the Academic Medical Center (other measurements). Plasma LH and FSH concentrations were analyzed on a Roche E170; intra- and interassay variations were <5%. Plasma T3 concentration was measured by in-house radioimmunoassay (RIA); intra- and interassay variations were 6.3% and 7.8%, respectively. FT4, FT3, TSH, prolactin and GH concentrations were analyzed by fluoroimmunoassay using the Delfia 1232 Fluorometer (PerkinElmer); intra- and interassay variations, respectively, were 5.1% and 6.8% (FT4), 7.7% and 11.3% (FT3), 4.2% and 5.7% (TSH), 3.4% and 5.3% (prolactin) and 3.8% and 6.2% (GH). Plasma testosterone concentration was analyzed by in-house RIA; intra- and interassay variations were 9.2% and 10.8%, respectively. Insulin was analyzed by chemiluminescence using Immulite 2000 (Siemens); intra- and interassay variations were 3.7% and 5.1%, respectively. Serum inhibin B and AMH concentrations were estimated using enzyme immunometric methods (Beckman Coulter). For AMH concentration, the Gen II assay was used; intra- and interassay variations were published previously[35,36].

Mouse pituitary TSH and PRL content measurement was previously described[37] and used reagents supplied by A.L. Parlow (National Hormone and Peptide Program). In Chicago, serum total T4 and T3 levels were measured by coated-tube RIA (Siemens Medical Solutions Diagnostics) adapted for mouse. TSH concentration was measured as previously described[38]. Free T4 levels were estimated from the ratio of total T4 to resin T4 uptake and expressed as the free T4 index (FT4I) as described[39].

Quantitative PCR. Mouse RNA was extracted from whole pituitaries and 3-mm hypothalamic blocks according to the following coordinates[40]: anteroposterior-interaural 3.94 to 0.94 mm, dorsoventral-interaural 2.5 mm and below, and 1.44 mm lateral. RNA (2 μg) was extracted and reverse transcribed as previously described[32]. Quantitative PCR (qPCR) was performed using Platinum SYBR Green qPCR SuperMix UDG (Invitrogen) and 0.4 pmol of each primer (**Supplementary Table 6**) on a Corbett Rotor-Gene 6200 HRM, using the manufacturer's protocol. Transcript levels were normalized to those of *Rpl19* (encoding ribosomal protein L19) and analyzed using the $2^{-\Delta\Delta CT}$ method[41,42].

Statistics. In **Figure 4** and all supplementary figures, statistical significance was defined as $P < 0.05$ and was determined by two-tailed Student's *t* test.

28. Li, H. & Durbin, R. Fast and accurate short read alignment with Burrows-Wheeler transform. *Bioinformatics* **25**, 1754–1760 (2009).
29. Li, H. *et al.* The Sequence Alignment/Map format and SAMtools. *Bioinformatics* **25**, 2078–2079 (2009).
30. Wu, T.D. & Nacu, S. Fast and SNP-tolerant detection of complex variants and splicing in short reads. *Bioinformatics* **26**, 873–881 (2010).
31. McKenna, A. *et al.* The Genome Analysis Toolkit: a MapReduce framework for analyzing next-generation DNA sequencing data. *Genome Res.* **20**, 1297–1303 (2010).
32. Bernard, D.J. Both SMAD2 and SMAD3 mediate activin-stimulated expression of the follicle-stimulating hormone β subunit in mouse gonadotrope cells. *Mol. Endocrinol.* **18**, 606–623 (2004).
33. Lanctôt, C., Gauthier, Y. & Drouin, J. Pituitary homeobox 1 (Ptx1) is differentially expressed during pituitary development. *Endocrinology* **140**, 1416–1422 (1999).
34. Gaston-Massuet, C. *et al.* Increased Wingless (Wnt) signaling in pituitary progenitor/stem cells gives rise to pituitary tumors in mice and humans. *Proc. Natl. Acad. Sci. USA* **108**, 11482–11487 (2011).
35. Siemensma, E.P., de Lind van Wijngaarden, R.F., Otten, B.J., de Jong, F.H. & Hokken-Koelega, A.C. Testicular failure in boys with Prader-Willi syndrome: longitudinal studies of reproductive hormones. *J. Clin. Endocrinol. Metab.* **97**, E452–E459 (2012).
36. Kevenaar, M.E. *et al.* Variants in the *ACVR1* gene are associated with AMH levels in women with polycystic ovary syndrome. *Hum. Reprod.* **24**, 241–249 (2009).
37. McGuinness, L. *et al.* Autosomal dominant growth hormone deficiency disrupts secretory vesicles *in vitro* and *in vivo* in transgenic mice. *Endocrinology* **144**, 720–731 (2003).
38. Pohlenz, J. *et al.* Improved radioimmunoassay for measurement of mouse thyrotropin in serum: strain differences in thyrotropin concentration and thyrotroph sensitivity to thyroid hormone. *Thyroid* **9**, 1265–1271 (1999).
39. Weiss, R.E. *et al.* Mice deficient in the steroid receptor co-activator 1 (SRC-1) are resistant to thyroid hormone. *EMBO J.* **18**, 1900–1904 (1999).
40. Paxinos, G. & Franklin, K.B.J. *The Mouse Brain in Stereotaxic Coordinates*, 2nd edn (Academic Press, San Diego, 2001).
41. VanGuilder, H.D., Vrana, K.E. & Freeman, W.M. Twenty-five years of quantitative PCR for gene expression analysis. *Biotechniques* **44**, 619–626 (2008).
42. Livak, K.J. & Schmittgen, T.D. Analysis of relative gene expression data using real-time quantitative PCR and the $2^{-\Delta\Delta CT}$ method. *Methods* **25**, 402–408 (2001).